

CrystEngComm

Accepted Manuscript



This is an *Accepted Manuscript*, which has been through the Royal Society of Chemistry peer review process and has been accepted for publication.

Accepted Manuscripts are published online shortly after acceptance, before technical editing, formatting and proof reading. Using this free service, authors can make their results available to the community, in citable form, before we publish the edited article. We will replace this *Accepted Manuscript* with the edited and formatted *Advance Article* as soon as it is available.

You can find more information about *Accepted Manuscripts* in the [Information for Authors](#).

Please note that technical editing may introduce minor changes to the text and/or graphics, which may alter content. The journal's standard [Terms & Conditions](#) and the [Ethical guidelines](#) still apply. In no event shall the Royal Society of Chemistry be held responsible for any errors or omissions in this *Accepted Manuscript* or any consequences arising from the use of any information it contains.

ARTICLE

Isomorphous free-base, Ni(II)- and Cu(II)-5,10,15,20-tetra(4-hydroxyphenyl)porphyrin nitrobenzene hexasolvates with tetragonal 3D hydrogen-bonded network structures

Cite this: DOI: 10.1039/x0xx00000x

Received 00th January 2012,
Accepted 00th January 2012

DOI: 10.1039/x0xx00000x

www.rsc.org/

Rüdiger W. Seidel^{*a} Richard Goddard^b and Iris M. Oppel^{*c}

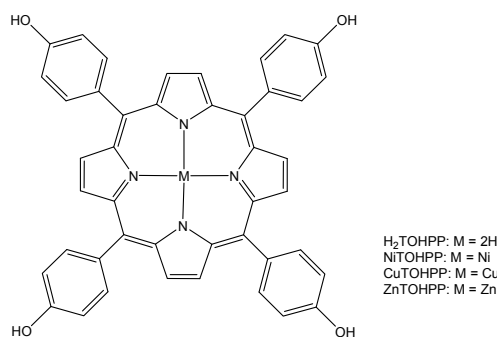
The crystal structures of 5,10,15,20-tetra(4-hydroxyphenyl)-21,23H-porphyrin nitrobenzene hexasolvate (**1**), 5,10,15,20-tetra(4-hydroxyphenyl)porphyrinatonicel(II) nitrobenzene hexasolvate (**2**) and 5,10,15,20-tetra(4-hydroxyphenyl)porphyrinatocopper(II) nitrobenzene hexasolvate (**3**) are described. Compounds **1–3** crystallise isomorphously in the non-centrosymmetric tetragonal space group $P4cc$ with $Z = 8$. There are three crystallographically distinct porphyrin molecules, two of which contain fourfold axes perpendicular to the porphyrin plane. The remaining one contains twofold axis perpendicular to the porphyrin ring system. The porphyrin building blocks are joined into a three-dimensional network through self-complementary O–H...O hydrogen bonding interactions between 4-hydroxyphenyl groups of adjacent molecules. The space occupied by the nitrobenzene solvent molecules is remarkably large at ca. 61.5 % of the unit cell volume in **1–3**.

Introduction

Supramolecular porphyrin solids have received much attention in the past two decades.^{1–9} The porphyrin macrocycle is an attractive scaffold for tailored building blocks for *crystal engineering* due to some unique features. The relatively rigid planar porphyrin ring system exhibits idealised D_{4h} symmetry, a point group rarely encountered in organic compounds. It can be readily functionalised for supramolecular self-assembly through coordinate bonds, hydrogen and halogen bonding.⁶ Furthermore, insertion of metal ions into the cavity of the porphyrin ring system enables tuning of redox properties and binding affinity for axial ligands, depending on the coordination preferences of the central metal.^{10,11}

5,10,15,20-Tetra(4-hydroxyphenyl)porphyrin (H_2TOHPP , Scheme 1) and its metalloderivatives are ideally suited as building blocks for hydrogen-bonded solids,⁶ since the four peripheral 4-hydroxyphenyl groups provide self-complementary hydrogen bonding sites. That means they can act as hydrogen bond donors and acceptors capable of forming hydrogen bonds to one another. Early investigations include those of $CuTOHPP$ and $ZnTOHPP$.^{12,13} Since d^{10} metalloporphyrins exhibit high binding affinity for one or two axial ligands, solvent molecules with oxygen donor atoms have frequently been found in axial coordination sites of

$ZnTOHPP$.^{12–14} Adducts of $ZnTOHPP$ and axial nitrogen donor ligands have also been studied.^{15–17} Interestingly, the hydroxyl groups of $ZnTOHPP$ approach axial coordination sites of adjacent molecules in the dimethylformamide solvate dihydrate, although competing oxygen donor solvent molecules are present.¹⁸ Attempts to prepare extended networks of H_2TOHPP peripherally linked by Gd(III) ions led to structural investigations of solvated discrete porphyrin-solvent assemblies of H_2TOHPP .¹⁹ Very recently, a number of solid-state hydrogen-bonded assemblies of H_2TOHPP and nitrogen bases as hydrogen bond acceptors have been presented.²⁰



Scheme 1 Chemical diagram of free-base 5,10,15,20-tetra(4-hydroxyphenyl)porphyrin and its Ni(II), Cu(II) and Zn(II) complexes.

The toluene trisolvate of ZnTOHPP [refcode in the Cambridge Structural Database (CSD):²¹ TEFURR] is an example of an MTOHPP-based open hydrogen-bonded network propagated solely by self-complementary hydrogen bonding interactions between the 4-hydroxyphenyl groups, without disruption by hydrogen-bonded solvent molecules.¹³ Motivated by these results, we investigated the self-assembly of H₂TOHPP, NiTOHPP and CuTOHPP in the presence of nitrobenzene as a crystallisation template. We chose d⁸ and d⁹ metalloporphyrins as building blocks in addition to the free-base porphyrin, since their low binding affinity for axial ligands¹¹ should help prevent undesired axial coordination by solvents molecules or 4-hydroxyphenyl groups of adjacent MTOHPP molecules. In this contribution, we report a structural study on nitrobenzene hexasolvates of H₂TOHPP, NiTOHPP and CuTOHPP.

Experimental

General

Starting materials were of reagent grade and used as received. H₂TOHPP was purchased from Porphyrin Systems (Appen, Germany). Solvents were of analytical grade and used without further purification. The metallation reactions of the free-base porphyrin were monitored by visible spectroscopy. Disappearance of the absorption bands of the free-base porphyrin indicated completion.^{22,23} NMR spectra of NiTOHPP (Figures S1 and S2, ESI) were recorded on a Bruker DRX 400 spectrometer, using dimethylsulfoxide-*d*₆ as solvent, and chemical shifts are reported relative to the residual solvent signals ($\delta_{\text{H}} = 2.50$ ppm, $\delta_{\text{C}} = 39.51$ ppm). Abbreviations: s (singlet), d (doublet). Fast atom bombardment (FAB) mass spectra (MS) were measured on a Fisons VG Autospec mass spectrometer, using 3-nitrobenzyl alcohol as a matrix.

Synthesis

NiTOHPP: H₂TOHPP (30 mg, 0.044 mmol) was dissolved in 5 mL of methanol and nickel(II) acetate tetrahydrate (110 mg, 0.440 mmol) was added. The reaction mixture was refluxed for 24 h. Subsequently, the mixture was poured into ethylacetate (30 mL) and washed three-times with deionised water. After drying on magnesium sulfate, the solvents were removed using a rotary evaporator. The product was dried over calcium chloride in vacuum. Yield: 29 mg (0.040 mmol, 91 %). MS(FAB): m/z 734 [M]⁺ (calcd. for C₄₄H₂₈N₄NiO₄). ¹H NMR(400.13 MHz): δ 9.87 (s, 4H; hydroxyl), 8.75 (s, 8H; β -pyrrole), 7.79 (d, $J = 8.4$ Hz, 8H; 2,6-phenyl), 7.13 (d, $J = 8.4$ Hz, 8H; 3,5-phenyl) ppm. ¹³C{¹H} NMR(100.62 MHz): 157.33 (4-phenyl), 142.29 (α -pyrrole), 134.56 (β -pyrrole), 132.01 (2,6-phenyl), 130.57 (1-phenyl), 118.88 (3,5-phenyl), 114.03 (*meso*) ppm.

CuTOHPP: H₂TOHPP (50 mg, 0.074 mmol) was dissolved in 5 mL of methanol and copper(II) acetate dihydrate (148 mg,

0.740 mmol) was added. The reaction mixture was stirred for 2 h at room temperature and worked up similarly to NiTOHPP. MS(FAB): m/z 739 [M]⁺ (calcd. for C₄₄H₂₈CuN₄O₄).

Crystallisation of 1–3: 10 mg (0.015 mmol) of H₂TOHPP were dissolved in 2 mL of methanol and 0.5 mL of nitrobenzene were added. The mixture was left at room temperature, while the solvent was allowed to evaporate slowly. A few red crystals of **1** were found after a couple of weeks. Reddish brown crystals of **2** were obtained from a solution of NiTOHPP in a mixture of acetonitrile, methanol and ethylacetate containing a few drops of nitrobenzene by slow evaporation of the solvent at room temperature. Red crystals of **3** were obtained from a solution of CuTOHPP in tetrahydrofuran containing a few drops of nitrobenzene by slow evaporation of the solvent at room temperature.

Single-crystal X-ray analysis

The X-ray intensity data for **1** were collected on a Bruker AXS Proteum X8 diffractometer, using Cu-K α radiation from a FR591 rotating anode with multilayer X-ray optics. The data collections for **2** and **3** were performed on an Oxford Diffraction Xcalibur2 diffractometer with a Sapphire2 CCD, using graphite-monochromated Mo-K α radiation. The data for **1** were integrated with SAINT²⁴ and corrected for absorption effects based on face-indexed Gaussian numerical integration and scaled with SADABS.²⁵ The data for **2** and **3** were processed with CrysAlisPro.²⁶ Absorption corrections based on multiple-scanned reflections were carried out with ABSPACK in CrysAlisPro.

The crystal structures were solved by direct methods with SHELXS-97 and refined with SHELXL-2014.²⁷ In order to increase the data/parameter ratio, the nitrobenzene solvent molecules were refined with isotropic atomic displacement parameters in **1–3**. Pairs of nitrobenzene molecules are disordered around fourfold axes in **1–3**. The benzene rings of these molecules were fitted as regular hexagons and standard similar distance restraints were applied to the nitro groups. Hydrogen atoms were placed at geometrically calculated positions and refined with the appropriate riding model and $U_{\text{iso}}(\text{H}) = 1.2 U_{\text{eq}}(\text{C}, \text{N}, \text{O})$. The positions of the hydroxyl and pyrrole hydrogen atoms were visible in difference Fourier maps, which were calculated with PLATON.²⁸ Nevertheless, disorder of the hydroxyl hydrogen atoms in **1–3** along the polar *c* axis direction cannot be ruled out in view of the rather limited precision of the structure analyses. In **1**, the core hydrogen atoms of the H₂TOHPP molecules containing fourfold rotation axes (Wyckoff positions 2a and 2b) are disordered by symmetry. Inspection of the difference Fourier map (Figure S3, ESI) indicated also disorder of the core hydrogen atoms of the H₂TOHPP molecules containing a twofold rotation axis (Wyckoff position 4c). Refinement of the ratio of occupancies of the two unique sites resulted in 0.7(1):0.3(1). Post-refinement calculation of the Flack parameter for **1** by Parsons's Q method²⁹ yielded a value of 0.3(1), which indicates that the crystal studied was an inversion twin. In the absence of a large anomalous signal, no twin refinement was carried out for **1**. The structures of **2** and **3** were refined as two-component inversion twins (using TWIN and BASF instructions), affording Flack parameters³⁰ of 0.42(4) and 0.45(5), respectively. Void estimations were performed with the SOLV routine in PLATON, using default options (grid step = 0.20 Å, probe

radius = 1.20 Å). Deviations from exact molecular point group symmetry were calculated with MOLSYM in PLATON. Representations of the crystal and molecular structures were drawn with MERCURY.³¹ Crystal data and refinement details are listed in Table 1.

Table 1 Crystal data and refinement details for 1–3.

(Place Table 1 here)

Results and discussion

H₂TOHPP was successfully metallated with Ni(II) and Cu(II), by applying the ‘acetate method’.²³ The experimental procedure was adapted from the synthesis of ZnTOHPP, reported by Smeets *et al.*³² Cu(II) could be readily inserted into the porphyrin core of H₂TOHPP at ambient conditions, similar to Zn(II). In contrast, insertion of Ni(II) required forced conditions, *i. e.* prolonged heating, since incorporation of Ni(II) into free-base porphyrins is kinetically hindered.¹⁰ Crystals of the nitrobenzene hexasolvates 1–3 were obtained by slow evaporation from solutions of H₂TOHPP, NiTOHPP and CuTOHPP in various solvents containing small amounts of nitrobenzene.

Single-crystal X-ray analysis revealed that 1–3 crystallise isomorphously in the tetragonal space group *P4cc*. In each case, the unit cell contains eight formula units (*Z* = 8). The porphyrin building blocks are located in special positions along the fourfold axes at (0,0,*z*), (0,0,*z*+1/2), Wyckoff position 2a, and (1/2,1/2,*z*), (1/2,1/2,*z*+1/2), Wyckoff position 2b, and the twofold axes at (0,1/2,*z*), (1/2,0,*z*), (0,1/2,*z*+1/2), (1/2,0,*z*+1/2), Wyckoff position 4c. The mean planes through the porphyrin moieties lie perpendicular to the symmetry axes, which are parallel to the polar *c* axis direction. Figure 1 shows a projection of the unit cell of 1 along the *c* axis and a diagram of symmetry operators of the space group *P4cc*. The asymmetric unit contains two distinct quarters and one half of a porphyrin unit and thus in sum one formula unit (*Z'* = 1), illustrating the limitation of the *Z'* notation for crystal structures in which the molecules occupy distinct special positions.³³

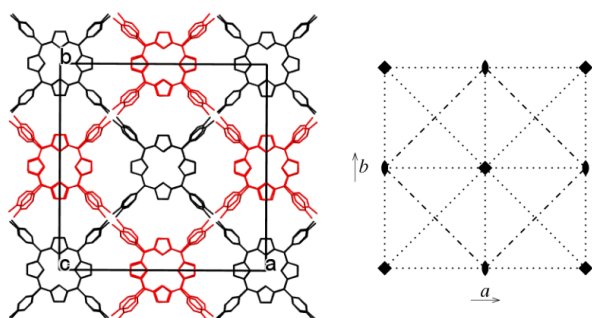


Fig 1 Left: The tetragonal unit cell of 1, viewed along the [001] direction. H₂TOHPP molecules with flat porphyrin core are shown in black (Wyckoff positions 2a and 2b) and those with ruffled core in red (Wyckoff position 4c). For sake of clarity, hydrogen atoms and nitrobenzene solvent molecules have been omitted. Right: Diagram of symmetry operators of the space group *P4cc*, projected along the same direction.

Figure 2 shows the structures of the MTOHPP molecules in Wyckoff positions 2a, 2b and 4c for 1–3 for the example of NiTOHPP in 2. Displacement ellipsoid plots of all distinct

MTOHPP molecules in 1–3 can be found in the Supporting Information (Figure S4, ESI). Table 2 lists selected geometric parameters in the porphyrins for 1–3. The 24-membered porphyrin macrocycles of the molecules in Wyckoff positions 2a and 2b are virtually flat with r.m.s. deviations in the range of 0.010–0.022 Å. In these molecules, the Ni atoms in 2 and the Cu atoms 3 are displaced from the porphyrin planes by no more than 0.020(5) Å. In contrast, the porphyrin macrocycles of the molecules that lie on the crystallographic twofold axes (Wyckoff position 4c) are *D*_{2d} ruffled (*ruf* deformation). In the core conformation termed *ruf*, opposite pyrrole rings are twisted so that the methine carbon atoms are alternately displaced above and below the mean plane through the porphyrin ring system.^{34,35} The extent of the *ruf* deformation can be characterised by the C_α–N···N–C_α torsion angle³⁶ (Scheme 2) or by the bisecting C_m···M···C_m angle for metalloporphyrins.³⁵ The 4-hydroxyphenyl substituents in the *meso* positions of the porphyrin rings adopt a propeller-like arrangement, regardless of whether the porphyrin is planar or ruffled. The dihedral angles between the mean planes of the phenyl rings and those of the porphyrins occur within the range of 62.8(2)–70.7(2)°. Bearing in mind that we cannot definitely rule out disorder of the hydroxyl hydrogen atoms (see Experimental Section), the hydroxyl groups all exhibit an *αααα* orientation,³⁷ *i. e.* the hydrogen atoms lie all above the porphyrin planes, as shown in Figure 2, along the polar *c* axis direction. The non-hydrogen atoms of the MTOHPP molecules in Wyckoff positions 2a and 2b exhibit r.m.s. deviations of 0.063–0.087 Å from exact *D*₄ point group symmetry in 1–3.

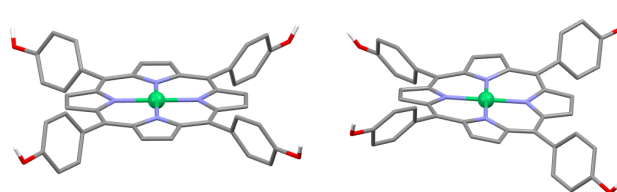
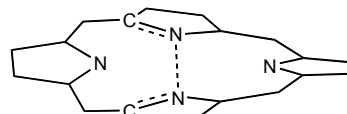


Fig 2 Molecular conformations of NiTOHPP in 2: flat (left) and *D*_{2d} ruffled (right) porphyrin core (*ruf* deformation). The Ni atoms are emphasised by a sphere. Carbon-bound hydrogen atoms are omitted for clarity.

Table 2 Selected geometric parameters (Å, °) in porphyrins for 1–3.

(Place Table 2 here)



Scheme 2 Definition of the C_α–N···N–C_α ruffling angle in the *ruf* conformation of the porphyrin macrocycle.³⁶

In 1, the NH hydrogen atoms of the H₂TOHPP molecules in Wyckoff positions 2a and 2b are necessarily disordered because of the site symmetry. For 5,10,15,20-tetraphenylporphyrin, it has been reasoned that the provision in a crystalline phase of sites that require or permit the molecules to observe statistically effective fourfold symmetry should be thermodynamically conducive to the dynamic type of disorder associated with the NH tautomerism.¹¹ The *ruf* conformer of H₂TOHPP in Wyckoff position 4c exhibits two crystallographically distinct pyrrole

rings. Inspection of the difference Fourier map (Figure S3, ESI) provided evidence for disorder of the NH hydrogen atoms between the two sites as well, but both the difference Fourier map and the unequal $C_{\alpha}-N-C_{\alpha}$ angles (Table 2, an increase is expected upon protonation) suggest that the two distinct NH sites are not equally occupied. The Ni(II) ions in **2** and the Cu(II) ions **3** are in a genuine square-planar coordination by the four pyrrole nitrogen atoms with $\Sigma(N-M-N)$ being close to the theoretical value of 720° for an ideal square-planar geometry, irrespective of the conformation of the porphyrin macrocycle. The M–N bond lengths are as expected for Ni(II) and Cu(II) porphyrins.¹¹

The coexistence of planar and *ruf* distorted cores each of H₂TOHPP, NiTOHPP and CuTOHPP in **1–3** raises the question as to whether the planar or *ruf* core conformation of H₂TOHPP, NiTOHPP and CuTOHPP is an intrinsic characteristic of the molecules or is a result of intermolecular interactions and close packing in the crystals. At the molecular level, a non-planar conformation generally disfavors π electron delocalisation in the porphyrin ring system, but some features of the planar conformation are nearly retained in the *ruf* conformation, viz. planarity of the pyrrole rings and a trigonal-planar structure at the α -pyrrole and *meso* carbon atoms. It is well documented that peripheral substituents in the *meso* and β -pyrrole positions and the metal ion in the cavity can cause a non-planar conformation.¹¹ An influence of the peripheral substituents can be ruled out in the case of **1–3**, since the coexisting planar and *ruf* conformers are chemically indistinguishable. Incorporation of metal ions that are too small for the porphyrin cavity can cause ruffled core conformations, as a result of shortened M–N bonds. It has been reported that a metal ion size of 2.035 Å ensures the best-fit in a planar porphyrin macrocycle.³⁵ For Ni(II) and Cu(II) porphyrins, the difference in energy for planar and *ruf* conformations is small; the planar conformer of 2,3,7,8,12,13,17,18-octaethylporphyrinatonicel(II) is marginally more stable than the *ruf* conformer by 1–1.5 kcal mol⁻¹.³⁵ Therefore, and because of the coexisting *ruf* conformer of the metal-free H₂OHTTP in **1**, we assume the *ruf* conformation observed for the MTOHPP molecules in Wyckoff position 4c in **1–3** is mainly a result of crystal forces. It is worth noting, however, that the extent of the *ruf* deformation is larger for NiTOHPP in **2** than for H₂TOHPP in **1** and CuTOHPP in **3**, as measured by the $C_{\alpha}-N\cdots N-C_{\alpha}$ torsion angles (Table 2). This could be associated with the smaller covalent radius of Ni [1.24(4) Å] with respect to Cu [1.32(4) Å]³⁸ and thus shorter Ni–N than Cu–N bonds. Flat and saddle-shaped core conformations of H₂TOHPP¹⁹ and ZnTOHPP with four-coordinated Zn(II)¹³ have been observed in various solvates. In the acetophenone tetrasolvate (CSD refcode: TEFREB), CuTOHPP adopts a flat core conformation.¹³ The porphyrin macrocycles in **1–3** are thus expected to exhibit some intrinsic flexibility.

The dominant intermolecular interactions in **1–3** are self-complementary O–H \cdots O hydrogen bonds between the hydroxyphenyl groups of adjacent MTOHPP molecules, consistent with Etter's general hydrogen bond rules for organic

compounds.³⁹ Hydrogen bonds between MTOHPP molecules and nitrobenzene solvent molecules are not observed. Indeed, the O \cdots O distances in **1–3** are remarkably similar, irrespective of whether they link planar to planar, planar to ruffled or ruffled to ruffled MTOHPP molecules and are close to the idealised distance in hexagonal ice (2.76 Å).⁴⁰ Columns of MTOHPP building blocks and edge-to-face stacked nitrobenzene molecules are interlinked along the symmetry axes parallel to the *c* axis direction by means of O–H \cdots O hydrogen bonds between the peripheral hydroxy-phenyl groups of the MTOHPP building blocks, thereby generating C₄¹(8) hydrogen-bonded chains⁴¹ at (1/4,1/4,z), (1/4,3/4,z), (3/4,1/4,z) and (3/4,3/4,z), which extend by translational symmetry in the polar *c* axis direction (Figure 4). The positions of the ruffled porphyrin cores lie in alternate columns (Figure 1a), suggesting that the *ruf* deformation occurs in order to accommodate the hydrogen bonds. The interstitial spaces between the porphyrin units, which are each displaced by *c*/2 (ca. 9.1 Å) along the *c* axis direction, are each occupied by six nitrobenzene molecules, which are sandwiched between, as shown in Figure 3. Since the seminal work by Robson and co-workers,⁴² nitrobenzene has been recognised to be particularly suited as a template to stabilise crystalline porphyrin assemblies with large solvent accessible voids.^{16, 43, 44} Exact knowledge of the arrangement of the nitrobenzene solvent molecules occupying these voids is often hampered by severe disorder. In **1–3**, the locations of the nitrobenzene molecules were established via difference Fourier syntheses and could be satisfactorily modelled. As shown in Figure 3, the nitrobenzene molecules are edge-to-face stacked with the aromatic porphyrin ring systems. Along the fourfold axes, the inner pairs of nitrobenzene molecules are disordered by symmetry, otherwise the pattern is repeated. To our knowledge and based on a search of the CSD, a similar arrangement of nitrobenzene and porphyrins in the solid-state to that observed in **1–3** is hitherto unknown. The resulting void occupied nitrobenzene solvent molecules is remarkably large at ca. 61.5 % per unit cell volume in **1–3**. By way of comparison, in the aforementioned ZnTOHPP toluene trisolvate (CSD refcode: TEFRUR), four-coordinate ZnTOHPP molecules form a centrosymmetric hydrogen-bonded network,¹³ and the crystal has a solvent occupied void of ca. 47.6 % of the unit cell volume. The porphyrin moieties are parallel and are separated by ca. 6.5 Å and accommodate face-to-face $\pi\cdots\pi$ stacked toluene solvent molecules.

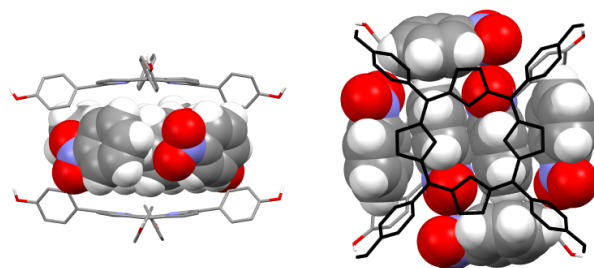


Fig 3 Lateral view (left) and top view (right), along the twofold axis, of an assembly of six nitrobenzene molecules sandwiched by two H₂TOHPP molecules (Wyckoff position 4c) in **1**. Nitrobenzene molecules are shown in space-filling representation. Hydrogen atoms of H₂TOHPP attached to carbon and nitrogen have been omitted for clarity.

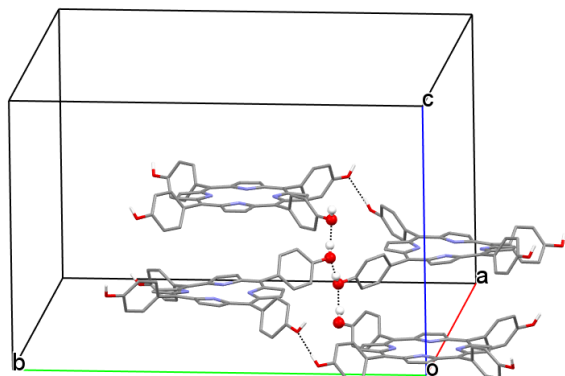


Fig 4 Section of the crystal structure of **1**, showing the linkage of four adjacent H₂TOHPP molecules via O–H...O hydrogen bonds (dashed lines). Hydroxyl groups forming a C₄(8) chain at (1/4,1/4,z) are highlighted by spheres. For the sake of clarity, only hydroxyl hydrogen atoms are shown and nitrobenzene solvent molecules have been omitted.

As described in the Experimental Section, the crystals of **1–3** studied were partial inversion twins, as is frequently observed for non-centrosymmetric crystals that are formed from building blocks without inherent chirality. Here, the twin operation changes the orientation of the structure and, thus, the arrangement of molecules and consequently the direction of the O–H...O hydrogen bonds with respect to the polar axis direction.⁴⁵ Fortuitously, the orientation of the major twin component in **1** and **2** corresponds to the minor component in **3**.

Conclusions

We have explored self-assembly of H₂TOHPP, NiTPPOH and CuTOHPP via hydrogen bonding interactions in the solid-state in the presence of nitrobenzene as a crystallisation template. Structural characterisation of the isomorphous nitrobenzene hexasolvates of H₂TOHPP, NiTPPOH and CuTOHPP (**1–3**) has been achieved. The results show that *meso* tetra(4-hydroxyphenyl)-substituted porphyrin building blocks are well suited for the construction of open three-dimensional hydrogen-bonded networks with polar if inversion twinned structures, under appropriate conditions. The nitrobenzene guest molecules adopt a unique structural arrangement in **1–3** and occupy a remarkable 61.5 % of the unit cell volumes, with distances between parallel porphyrin planes of ca. 9.1 Å. In accord with previous studies, coexisting MTOHPP molecules with flat and ruffled porphyrin cores in **1–3** reveal some intrinsic conformational flexibility.

Acknowledgements

This work was funded by the Deutsche Forschungsgemeinschaft (DFG). We would like to thank Dr Wanning Hu for assistance in preparing the samples studied and Gregor Barchan

for recording the NMR spectra. R. W. S. is grateful to Professor Christian W. Lehmann for his support of this project.

Notes and references

^a Lehrstuhl für Analytische Chemie, Ruhr-Universität Bochum, Universitätsstraße 150, 44780 Bochum, Germany. E-Mail: Ruediger.Seidel@rub.de; Fax: +49 234 32 14420; Tel: +49 234 32-28194

^b Max-Planck-Institut für Kohlenforschung, Kaiser-Wilhelm-Platz 1, 45470 Mülheim an der Ruhr, Germany.

^c Institut für Anorganische Chemie, Rheinisch-Westfälische Technische Hochschule Aachen, Landoltweg 1, 52074 Aachen, Germany. E-Mail: iris.oppel@ac.rwth-aachen.de; Fax: +49 241 80 92 644; Tel: +49 241 80 94 645

† Dedicated to Professor Wolfgang Lubitz on the occasion of his 65th birthday.

Electronic Supplementary Information (ESI) available: Fig. S1–S4. CCDC 1024148–1024150 for **1–3**. See DOI: 10.1039/b000000x/

- 1 I. Goldberg, *Chem. Eur. J.*, 2000, **6**, 3863–3870.
- 2 K. S. Suslick, N. A. Rakow, M. E. Kosal, J. H. Chou, *J. Porphyrins Phthalocyanines*, 2000 **4**, 407–413.
- 3 I. Goldberg, *Chem. Commun.*, 2005, 1243–1254.
- 4 K. S. Suslick, P. Bhyrappa, J.-H. Chou, M. E. Kosal, S. Nakagaki, D. W. Smithenry, S. R. Wilson, *Acc. Chem. Res.*, 2005, **38**, 283–291.
- 5 C. M. Drain, I. Goldberg, I. Sylvain, A. Falber, *Top. Curr. Chem.*, 2005, **245**, 55–88.
- 6 I. Goldberg, *CrystEngComm*, 2008, **10**, 637–645.
- 7 C. Zou, C.-D. Wu *Dalton Trans.*, 2012, **41**, 3879–3888.
- 8 B. J. Burnett, P. M. Barrona, W. Choe, *CrystEngComm*, 2012, **14**, 3839–3846.
- 9 W.-Y. Gao, M. Chrzanowski, S. Ma, *Chem. Soc. Rev.*, 2014, **43**, 5841–5866.
- 10 P. Hambright, in *Porphyrins and Metalloporphyrins*, ed. K. M. Smith Elsevier, Amsterdam, 1975, pp. 233–278.
- 11 J. L. Hoard, in *Porphyrins and Metalloporphyrins*, ed. K. M. Smith, Elsevier, Amsterdam, 1975, pp. 317–380.
- 12 M. P. Byrn, C. J. Curtis, Y. Hsiou, S. I. Khana, P. A. Sawin, S. K. Tendick, A. Terzis, C. E. Strouse, *J. Am. Chem. Soc.*, 1993, **115**, 9480–9497.
- 13 I. Goldberg, H. Krupitsky, Z. Stein, Y. Hsiou, C. E. Strouse, *Supramol. Chem.*, 1994, **4**, 203–221.
- 14 Y. Diskin-Posner, G. K. Patra, I. Goldberg, *Acta Cryst.*, 2002, **C58**, m344–m346.
- 15 Y. Diskin-Posner, G. K. Patra, I. Goldberg, *Chem. Commun.*, 2002, 1420–1421.
- 16 Y. Diskin-Posner, G. K. Patra, I. Goldberg, *CrystEngComm*, 2002, **4**, 296–301.
- 17 M. Vinodu, I. Goldberg, *New J. Chem.*, 2004, **28**, 1250–1254.
- 18 V. E. de Oliveira, C. C. Correa, C. B. Pinheiro, R. Diniza, L. F. C. de Oliveira, *J. Mol. Struct.*, 2011, **995**, 125–129.
- 19 S. Lipstman, I. Goldberg, *Acta Cryst.*, 2009, **C65**, o3–o7.
- 20 P. Nandy, V. Pedireddi, *Acta Cryst.*, 2014, **A70**, C554.
- 21 C. R. Groom, F. H. Allen, *Angew. Chem. Int. Ed.*, 2014, **53**, 662–671.
- 22 M. Gouterman, *J. Mol. Spectrosc.*, 1961, **6**, 138–163.

- 23 J. W. Buchler, in *Porphyrins and Metalloporphyrins*, ed. K. M. Smith, Elsevier, Amsterdam, 1975, pp. 157-231.
- 24 SAINT, Bruker AXS Inc., Madison, Wisconsin, USA, 2007.
- 25 SADABS, Bruker AXS Inc., Madison, Wisconsin, USA, 2001.
- 26 CrysAlisPro, version 1.171.37.34, Agilent Technologies UK Ltd, Oxford, UK, 2014.
- 27 G. M. Sheldrick, *Acta Cryst.*, 2008, **A64**, 112–122.
- 28 A. L. Spek, *Acta Cryst.*, 2009, **D65**, 148–155.
- 29 S. Parsons, H. D. Flack, T. Wagner, *Acta Cryst.*, 2013, **B69**, 249–259.
- 30 H. D. Flack, *Acta Cryst.*, 1983, **A39**, 876–881.
- 31 C. F. Macrae, I. J. Bruno, J. A. Chisholm, P. R. Edgington, P. McCabe, E. Pidcock, L. Rodriguez-Monge, R. Taylor, J. van de Streek, P. A. Wood, *J. Appl. Cryst.*, 2008, **41**, 466–470.
- 32 S. Smeets, H. Roex, W. Dehaen, *ARKIVOC*, 2003, 83–92.
- 33 A. D. Bond, *CrystEngComm* 2008, **10**, 411–415.
- 34 W. R. Scheidt, Y. J. Lee, *Struct. Bond.*, 1987, **64**, 1–70.
- 35 O. Q. Munro, J. C. Bradley, R. D. Hancock, H. M. Marques, F. Marsicano, P. W. Wade, *J. Am. Chem. Soc.*, 1992, **114**, 7218–7230.
- 36 A. Ghosh, T. Wondimagegn, E. Gonzalez, I. Halvorsen, *J. Inorg. Biochem.*, 2000, **78**, 79–82.
- 37 A. C. Tome, A. M. S. Silva, I. Alkorta, J. Elguero, *J. Porphyrins Phthalocyanins*, 2011, **15**, 1–28.
- 38 B. Cordero, V. Gomez, A. E. Platero-Prats, M. Reves, J. Echeverria, E. Cremades, F. Barragana, S. Alvarez, *Dalton Trans.*, 2008, 2832–2838.
- 39 M. C. Etter, *Acc. Chem. Res.*, 1990, **23**, 120–126.
- 40 W. F. Kuhs, M. S. Lehmann, *J. Phys. Chem.*, 1983, **87**, 4312–4313.
- 41 J. Bernstein, R. E. Davis, L. Shimon, N.-L. Chang, *Angew. Chem. Int. Ed.*, 1995, **34**, 1555–1573.
- 42 B. F. Abrahams, B. F. Hoskins, D. M. Michail, R. Robson, *Nature*, 1994, **369**, 727–729.
- 43 Y. Diskin-Posner, I. Goldberg, *Chem. Commun.*, 1999, 1961–1962.
- 44 M. Vinodu, I. Goldberg, *CrystEngComm*, 2005, **7**, 133–138.
- 45 P. G. Jones, *Acta Cryst.*, 1986, **A42**, 57.

Table 1 Crystal data and refinement details for **1–3**.

	1	2	3
Empirical formula	C ₈₀ H ₆₀ N ₁₀ O ₁₆	C ₈₀ H ₅₈ N ₁₀ NiO ₁₆	C ₈₀ H ₅₈ CuN ₁₀ O ₁₆
M_r	1417.38	1474.07	1478.90
λ (Å)	1.54178	0.71073	0.71073
Crystal size (mm ³)	0.49 × 0.08 × 0.05	0.33 × 0.27 × 0.18	0.34 × 0.14 × 0.07
Crystal system	tetragonal	tetragonal	tetragonal
Space group	<i>P4cc</i>	<i>P4cc</i>	<i>P4cc</i>
T (K)	100(2)	108(2)	108(2)
a (Å)	27.452(1)	27.3385(7)	27.3921(7)
c (Å)	18.2099(8)	18.3255(8)	18.3185(9)
V (Å ³)	13723(1)	13696.4(9)	13745(1)
Z	8	8	8
ρ_{calc} (g cm ⁻³)	1.372	1.430	1.429
μ (mm ⁻¹)	0.806	0.365	0.399
$F(000)$	5904	6112	6120
θ range (°)	1.609 – 55.262	3.513 – 26.368	3.484 – 23.256
Reflections collected / unique	180455 / 8581	80726 / 13993	99874 / 9857
R_{int}	0.0629	0.1661	0.2216
Observed reflections [$I > 2\sigma(I)$]	7944	7301	5969
Goodness-of-fit on F^2	1.036	1.020	1.024
Parameters / restraints	698 / 9	709 / 9	709 / 9
R_1 [$I > 2\sigma(I)$]	0.0776	0.0781	0.0769
wR_2 (all data)	0.2099	0.2180	0.2131
Residuals (eÅ ⁻³)	0.754 / -0.430	1.497 / -0.484	1.403 / -0.456

Table 2 Selected geometric parameters (Å, °) in porphyrins for **1–3**.

Porphyrin ^a	1			2			3		
	H ₂ TOHPP (2a)	H ₂ TOHPP (2b)	H ₂ TOHPP (4c)	NiTOHPP (2a)	NiTOHPP (2b)	NiTOHPP (4c)	CuTOHPP (2a)	CuTOHPP (2b)	CuTOHPP (4c)
Site symmetry	C ₄	C ₄	C ₂	C ₄	C ₄	C ₂	C ₄	C ₄	C ₂
M–N	–	–	–	1.958(8)	1.953(8)	1.956(8)	2.01(1)	2.00(1)	2.00(1)
						1.944(7)			2.00(1)
N–M–N	–	–	–	90.0	90.0	90.1(3)	90.0	90.0	89.5(4)
				179.8(6)	179.9(6)	89.9(3)	179.5(8)	179.4(8)	90.4(4)
						178.0(6)			177.9(8)
						179.4(6)			178.4(8)
C _α –N–C _α	107.8(6)	107.6(6)	106.2(6)	103.4(8)	104.5(8)	104.6(8)	105(1)	106(1)	105(1)
			109.0(6)			104.8(8)			107(1)
C _m ···M···C _m	–	–	–	179.9(3)	179.3(3)	171.1(2)	179.9(4)	178.8(4)	172.1(3)
						171.1(2)			173.5(3)
C _α –N···N–C _α	–0.5(9)	0.1(9)	12.2(9)	–1(1)	1(1)	16(1)	0(2)	0(2)	–13(2)
			–12.4(9)			–17(1)			14(2)